Facile Route to Synthesize Multiwalled Carbon Nanotube/Zinc Sulfide Heterostructures: Optical and Electrical Properties

Jimin Du, Lei Fu, Zhimin Liu, Buxing Han,* Zhonghao Li, Yunqi Liu,* Zhenyu Sun, and Daoben Zhu

Center for Molecular Sciences, Institute of Chemistry, Chinese Academy of Sciences, Beijing 100080, China

Received: March 11, 2005; In Final Form: May 12, 2005

A simple method to decorate the multiwalled carbon nanotubes (MWCNTs) with ZnS nanospheres has been developed. The method involves ultrasonic pretreatment and heat treatments of MWCNTs, zinc chloride, and thiourea in ethanol. The heterostructures have been characterized by X-ray diffraction (XRD), scanning electron microscopy (SEM), and transmission electron microscopy (TEM). Comparative experiments show that both ultrasonic treatment and heat treatment are necessary for synthesizing the MWCNTs/ZnS heterostructures. Moreover, a photoluminescence spectrum shows that the MWCNTs/ZnS heterostructures feature a broad blue emission at about 430 nm, indicating that there exists significant ground-state interaction between ZnS nanospheres and MWCNTs. Meanwhile, the current−voltage characteristic of the MWCNTs/ZnS exhibits clear rectifying behavior, revealing charge transfer between MWCNTs and ZnS nanospheres.

Introduction

Low-dimensional materials in the forms of tubes, wires, and belts represent a broad class of nanometer-scale building blocks with novel properties in comparison with bulk materials.[1] Recently, low-dimensional materials, such as carbon nanotubes,[2] Si nanowires,[3] ZnO nanowires,[4] ZnS nanowires,[5] and SnO_2 nanobelts,[6] have been widely studied for their potential applications in electronic and optical devices. Among them, carbon nanotubes (CNTs) are one of the most attractive nanomaterials, primarily due to their unique physicochemical properties and wide potential applications in nanoelectronics,[7] nanolithography,[8] sensing,[9] and high-resolution imaging.[10] With the successful production of CNTs in large scales, it is desirable to further open their application fields. CNTs decorated with organic and inorganic compounds through covalent and noncovalent bonds can provide new properties and may lead to new applications. Covalent modification of carbon nanotube sidewalls includes mainly oxidation, fluorination, and formation of amide bonds.[11] Noncovalent approaches utilize π-stacking or van der Waals interactions between functional compounds and CNTs.[12] Recently, noncovalent functionaliztion of carbon nanotubes has attracted more attention because it can be expected to present nanocomposites with new properties while still preserving nearly all the properties of the nanotubes.

Many efforts have been focused on functionalization of CNTs to form CNT−nanoparticle heterojunctions with an intrinsically configurable moiety.[13a−f] One such structure is the family of semiconductor nanocrystals, which exhibits excellent optical and electrical properties. For example, Krauss et al. attached CdSe core and CdSe/ZnS core/shell quantum dots to single walled carbon nanotubes (SWNTs) via an amide-coupling scheme.[14] Wong et al. synthesized functional SWNTs covalently joined to CdSe and TiO_2 semiconductor nanocrystals by short chain organic molecule lingers.[15] More recently, we decorated MWCNTs with Co_3O_4 beads via heating cobalt nitrate in supercritical carbon dioxide modified with ethanol cosolvent.[16] Functionalization of CNTs can provide the nanocomposites with new properties, which result either from the functional groups or from the synergetic effects of the functional groups and CNTs. Thus, as the demand for smaller and faster electronic devices increases, functional CNTs may play an important role in the miniaturization process of nanoengineering and nanotechnology, including nanotransistors, nanobatteries, and nanosensors, etc.

ZnS is one of the most important semiconductors in optical devices due to the high index of refraction and a high transmittance in the visible range.[17] Functionalizing CNTs with ZnS nanospheres can not only combine the advantages of ZnS and CNTs but also may result in new properties, which have potential applications in the nanoscale electronic devices. In this paper, we report a simple method to decorate MWCNTs with ZnS nanospheres to form MWCNTs/ZnS heterostructures. The heterostructures demonstrate that there is a significant ground-state interaction between ZnS nanospheres and MWCNTs, and the herterostructures exhibit obvious rectifying behavior.

Experimental Procedures

The MWCNTs with a purity of about 95% were provided by Shenzhen Nanoprot Company, which was produced via catalytic decomposition of CH_4.[18] In a typical experiment to prepare the MWCNTs/ZnS herterostructures, about 9 mg of MWCNTs, 1 mmol of zinc chloride, and 1 mmol of thiourea were added to 12 mL of ethanol. The reaction mixture was treated under ultrasonication (100 W, 40 kHz) for 30 min. Then, the mixture was moved to a stainless steel autoclave of 22 mL. After it was sealed, the autoclave was heated to 180 °C for about 12 h, resulting in the MWCNTs/ZnS herterostructures. The as-obtained samples were washed with deionized water and ethanol 3 times under the aid of the ultrasonacation, respectively. Then, the products were obtained by centrifugation at 4000 rpm. The products were dried at 50 °C in a vacuum oven before being further characterized. We also carried out parallel experiments only by ultrasonic treatment or heat treatment at 20, 80, and 140 °C, respectively, and other conditions were the same.

The X-ray diffraction (XRD) patterns of the samples were obtained on a powder X-ray diffractometer (D/Max 2550 V, Rigaku, Japan) using Kα radiation ($\lambda = 1.5418$ Å). The scanning electron microscopy (SEM) images were taken on a JEOL JSM-

10.1021/jp051284i CCC: $30.25
Published on Web 06/11/2005

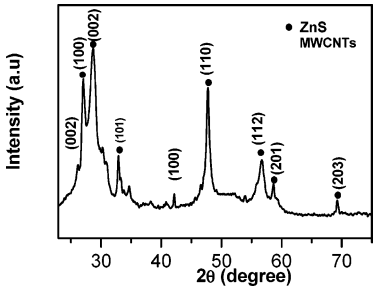

Figure 1. XRD spectrum of the MWCNTs/ZnS composites.

6700F SEM. Transmission electron microscopy (TEM, JEM 2010, JEOL, Japan) was performed to observe the microstructure of the composites. Selected area electronic diffraction (SAED) was also taken on the same apparatus. A photoluminescence (PL) spectrum was recorded on a Shimadzu RF-5301 PC spectrofluorophotometer at room temperature. The electrical properties of the MWCNTs/ZnS herterostructures were measured using Probe Station (Wentworth Company MP1008) and Semiconductor Parameter Analyzer (Hewlett-Packard 4140B) at room temperature in air.

Results and Discussion

XRD Patterns of the Products. Figure 1 shows the XRD patterns of the MWCNTs/ZnS sample. The peaks centered at 26 and 44° correspond to (002) and (100) reflections of graphite from the MWCNTs, respectively.[19] Strong diffraction peaks appearing at about 27, 28, and 47° are attributed to the (100), (002), and (110) planes of the wurtzite structure phase of ZnS.[20] The average size of the ZnS particles was determined from the width of the reflection according to the Debye−Scherrer equation.[21]

$$D = \frac{0.9\lambda}{\beta \cos \theta} \tag{1}$$

where β is the full width at half-maximum (fwhm) of the peak, θ is the angle of diffraction, and λ is the wavelength of X-ray radiation. To obtain a more accurate fwhm value, the deconvolutions of the signals of the (002) and (110) reflections were measured to be 1.26 and 0.84°, respectively, and the mean sizes calculated were 38 and 41 nm, respectively. These sizes are much smaller than those observed from the SEM observation, which is about 180 nm. Therefore, it can be concluded that the ZnS particles must be composed of smaller crystals.

Morphologies of the MWCNTs/ZnS Heterostructures. The MWCNTs are randomly decorated with a large quantity of ZnS nanospheres with a relatively uniform diameter of about 180 nm, as can be known from the SEM image in Figure 2a. The nanospheres are composed of ZnS flakes, which are assembled to form the surface of the nanospheres. The low magnification TEM image (Figure 2b) also shows that the MWCNTs exhibit the heterostructure with ZnS nanospheres along the MWCNTs outer surface. In the growing process of ZnS nanoshpheres, the MWCNTs may act as a template, which limits the produced ZnS particles to access each other, thereby forming quasi-one-dimensional ZnS nanospheres along MWCNTs.

A typical TEM image indicates that ZnS nanospheres are attached to the outmost and that the MWCNTs are located in the middle of the ZnS nanospheres, as observed in Figure 2c. The selected area electron diffraction (SAED) (Figure 2c inset) shows diffraction rings, indicating that the produced ZnS nanospheres are polycrystalline. The two inside track diffraction rings correspond to (111) and (220) reflections of wurtzite structure phase ZnS, respectively, which is consistent with the XRD results. Detailed microstructure information of the ZnS nanospheres is further characterized by high-resolution TEM (Figure 2d), which shows well-defined lattice fringes of ZnS flakes, illustrating that each of the flakes is a single crystal. The measured spacing of the crystallographic planes is 0.312 nm (inset a shown in Figure 2d) and 0.335 nm (inset b shown in Figure 2d) from the HRTEM images, corresponding to the [111] and [100] lattice planes of the wurtzite structure ZnS crystal, respectively, which are consistent with the reported *d* spacing values.[22] The MWCNTs used in this work exhibit an interlayer spacing of 0.34 nm (inset c shown in Figure 2d), which corresponds to the interplanar distance of the (002) planes of graphite.[23]

To control the size and morphology of ZnS nanoparticles, similar experiments were carried out with the aid of the ultrasonication without heating treatment and with heating treatment at 80 and 140 °C for 12 h, and the SEM images are shown in Figure 3. The outer surface of the MWCNTs turned relatively rough after the ultrasonication treatment at room temperature (Figure 3a) in comparison with that of pristine MWCNTs (not shown), which might result from the formation of very small ZnS clusters adhering to the exterior surface of the MWCNTs. When the heat treatment temperature was increased to 80 °C, the ZnS particles became larger as shown in Figure 3b. By closer observation, some of ZnS particles feature the half-baked and fractal structure due to the low temperature. In a further increase of reaction temperature to 140 °C (Figure 3c), ZnS particles exhibited quasi-sphere structure, and the size was larger than that of the products obtained at 80 °C. The ZnS spheres were nearly coated on the MWCNTs surface to form MWCNTs/ZnS heterostructures. The MWCNTs/ZnS heterostructures obtained at 180 °C (Figure 2) were more uniform in comparison with the products obtained at 80 and 140 °C, indicating that the reaction temperature had an important effect on the morphology of the MWCNTs/ZnS heterostructures. Meanwhile, the similar experiment was also conducted at 180 °C without the ulatrasonication pretreatment, and the SEM image (Figure 3d) showed that most of the ZnS spheres was not adhering to the MWCNTs surface. This might result from the lack of the ZnS clusters formed on the MWCNTs surface during the ultrasonication pretreatment, illustrating that the ultrasonication also played an important role in preparing the uniform MWCNTs/ZnS heterostructures. We also carried out the experiments in the absence of the MWCNTs at 180 °C with ultrasonication pretreatment, whose rersults demonstrated that ZnS spheres with a diameter of about 400 nm were obtained as shown in Figure 3e.

Possible Formation Mechanism and Influence Factors. On the basis of our experimental results, MWCNTs were functionalized with semiconductive ZnS nanospheres with the aid of the ultrasonic and heating treatment at 180 °C. On the basis of our comparative facts, both ultrasonic and heat treatment play an important role in synthesizing MWCNTs/ZnS heterostructures. Therefore, we propose the growth mechanism of MWCNTs/ZnS herterostructures as follows:

$$\text{EtOH})))) \ H^{\bullet} + \text{EtO}^{\bullet} \tag{1}$$

$$2H^{\bullet} + RS \rightarrow H_2S + R^{\bullet} (RS = H_2NCSNH_2) \tag{2}$$

$$S^{2-} + Zn^{2+} \rightarrow ZnS \tag{3}$$

$$n(\text{ZnS}) + \text{MWCNTs} \rightarrow \text{MWCNTs/ZnS} \tag{4}$$

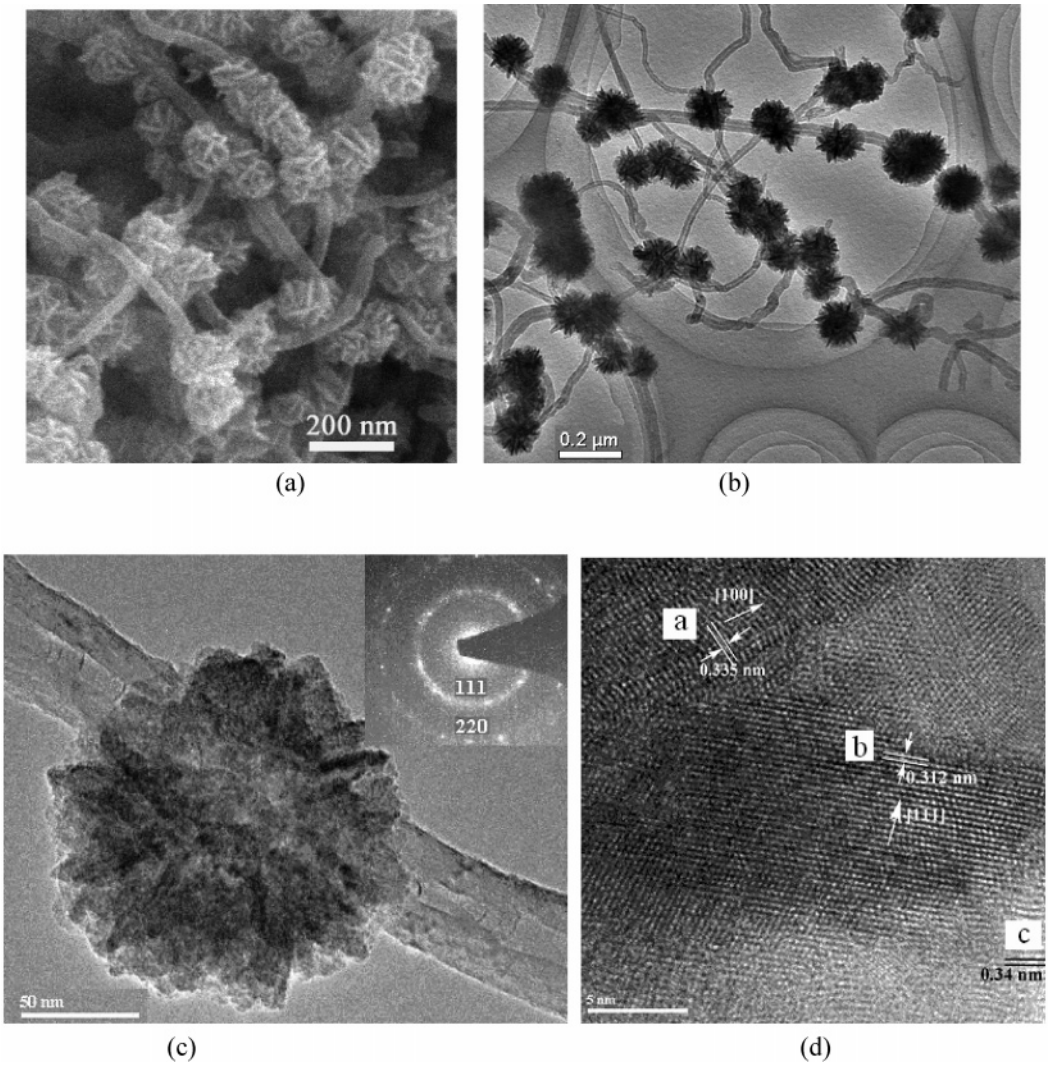

Figure 2. (a) SEM images of the MWCNTs/ZnS herterostructures. (b) TEM images of low magnification. (c) Typical MWCNTs/ZnS herterostructures. Inset: SEAD patterns of ZnS nanospheres. (d) High magnification TEM images.

Equation 1 represents the formation of radicals ($H^{\bullet}$ and $EtO^{\bullet}$) from ethanol with the aid of the ultrasonic waves.[24] Equations 2 and 3 represent the main reactions leading to the formation of ZnS clusters in solution.[24] In view of the low-energy point, the initially generated ZnS may attach to the surface of MWCNTs to form small ZnS clusters. Then, the smaller clusters can act as nuclei for the particle growth via the Oswald ripening process in the subsequent heat treatment.[25] Therefore, a combination of the ultrasonic treatment and the heat treatment is necessary to the formation of the MWCNTs/ZnS hertero-structures.

Photoluminescence (PL) Spectrum. Recently, it has been reported that CNTs can act as good electron acceptors and that charge transfer has been magnified in the CNT-based composite system.[26] Furthermore, CNTs can act as energy sinks in an excited-state energy transfer mechanism due to the effect of the electron acceptors of CNTs.[27] In our experiments, the optical property of the resulting MWCNTs/ZnS heterostructures was determined by means of PL analysis. Figure 4 gives the photoluminescence (PL) spectrum of the pristine MWCNTs, ZnS spheres of the diameter of about 400 nm (Figure 3e), and MWCNTs/ZnS heterostructure, respectively. The MWCNTs do not have emission peaks (Figure 4a). The ZnS spheres have weak emission peaks centered about 435 nm (Figure 4b),[28] while the MWCNTs/ZnS heterostructure features a blue emission at around 430 nm (Figure 4c), which is associated with defect-related emission of the ZnS nanospheres. It is also noted that the PL spectral response is relatively broad, indicating that there is a significant ground-state interaction between ZnS nanospheres and MWCNTs.[29] It can be concluded that electrons from the external ZnS nanospheres will flow into the inner MWCNTs, forming an accumulation layer of electrons. This suggests that the MWCNTs/ZnS heterosturctures may find applications for highly efficient photoelectrochemical cells, as recent work showed with a CNT/CdS core/shell composite.[30] On the other hand, size and shape of ZnS particles are not uniform, which also results in the wide band.

Electrical Properties of the MWCNTs/ZnS Heterostructures. CNTs have unique electrical properties, making them prime candidates for applications in nanoelectronics.[31] Among these, electronic devices have attracted considerable interest since they are ideal devices for high precision electrometry.[32] To date, many researchers elaborately studied the decorated CNTs field effect.[33] In this paper, the electrical properties of the MWCNTs/ZnS heterostructures were studied by applying the probe station and semiconductor parameter analyzer. To fabricate the diodes, the MWCNTs/ZnS heterostructrues were spread on a 500 nm thick thermal oxidized silicon surface between the Ti/Au pads. Using a probe point extension focused-ion-beam (FIB) system, the surface was visualized using a low beam current (4 pA) in searching for the nanotubes. One Pt lead was patterned on the ZnS nanospheres, and the other was patterned on the MWCNTs

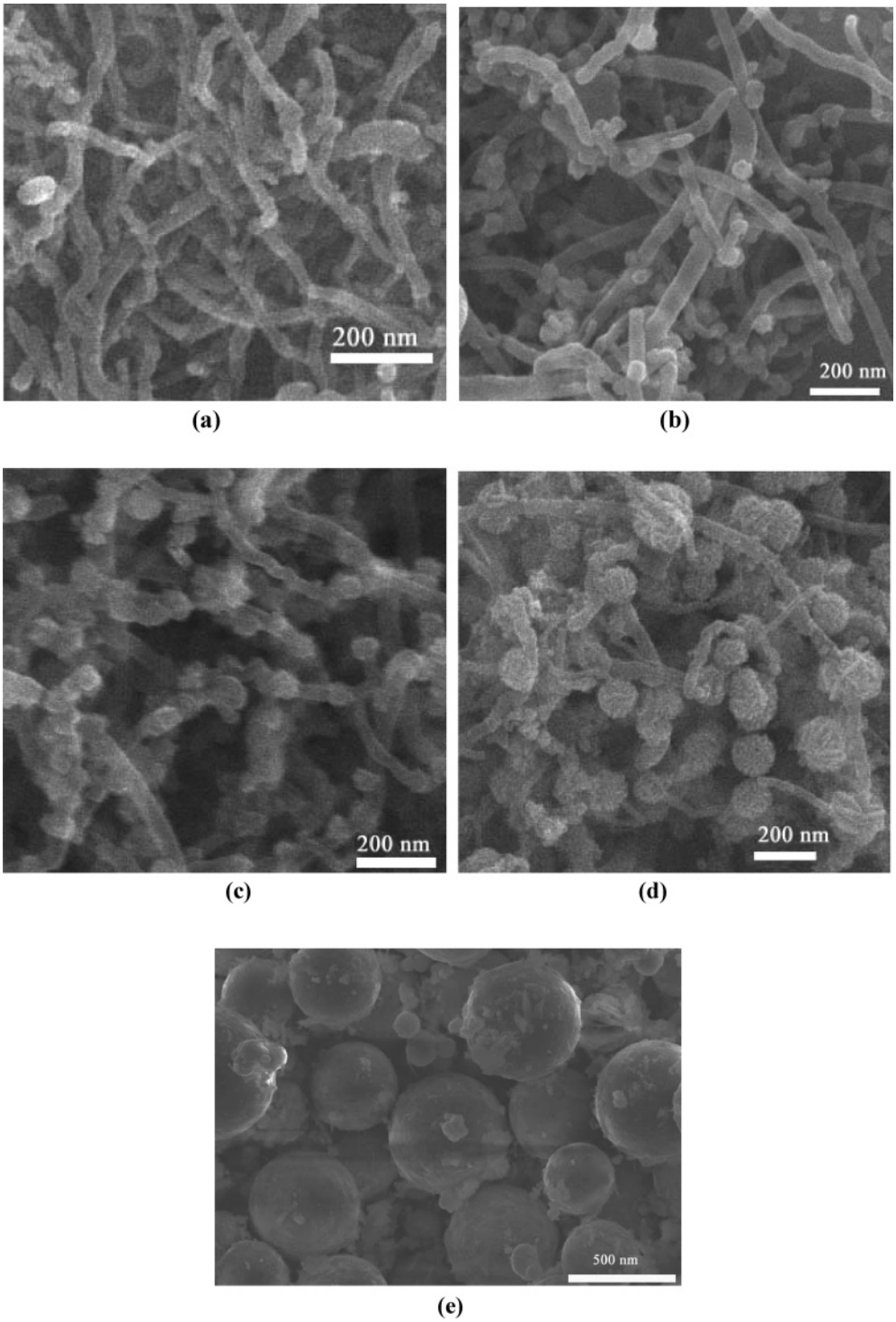

Figure 3. (a−c) SEM images of MWCNTs/ZnS heterostructures synthesized with the aid of the ultrasonic and heating treatment at 20, 80, and 140 °C, respectively. (d) SEM images of MWCNTs/ZnS heterostructures synthesized without the aid of the ultrasonacation at 180 °C. (e) ZnS spheres prepared in the absence of the MWCNTs.

(diameter of the Pt leads was 50 nm). The resulting connections are shown in Figure 5a. The right inset SEM image is the morphology of the decorated MWCNTs before patterning leads (inset a inset in Figure 5a). These small leads were then connected to surrounding Au/Ti pads. The left inset is the schematic diagram illustrating the framework of the device. The electrical properties were measured using the probe station and semiconductor parameter analyzer at room temperature in the air. To obtain better contact, the thermal annealing was performed in a flowing Ar atmosphere at 400 °C for 20 min using a tube furnace. Figure 5b shows the current−voltage ($I-V$) characteristic of the MWCNTs and MWCNTs/ZnS heterostructures at room temperature, respectively. The $I-V$ characteristics of the MWCNTs are linear, showing that the MWCNTs present metallic characteristics,[34] while the MWCNTs/ZnS heterostructure exhibits clear rectifying behaviors, which shows the *n*-type semiconductor characteristics.[35] The rectifying mechanism is similar to that of a conventional PN junction.[36] The ZnS nanospheres attached to the MWCNTs can cause a shift of the Fermi level toward the conduction band by electron donation, leading to a $p/p(-)$ junction in the nanotube. The current flowing as forward bias lowers the potential barrier

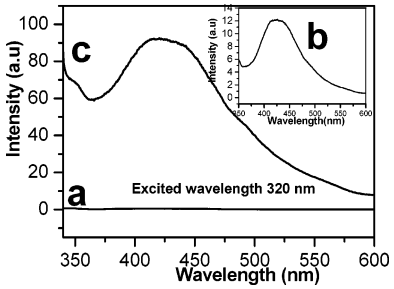

Figure 4. PL spectrum of (a) MWCNTs, (b) ZnS spheres, and (c) MWCNTs/ZnS heterostructures.

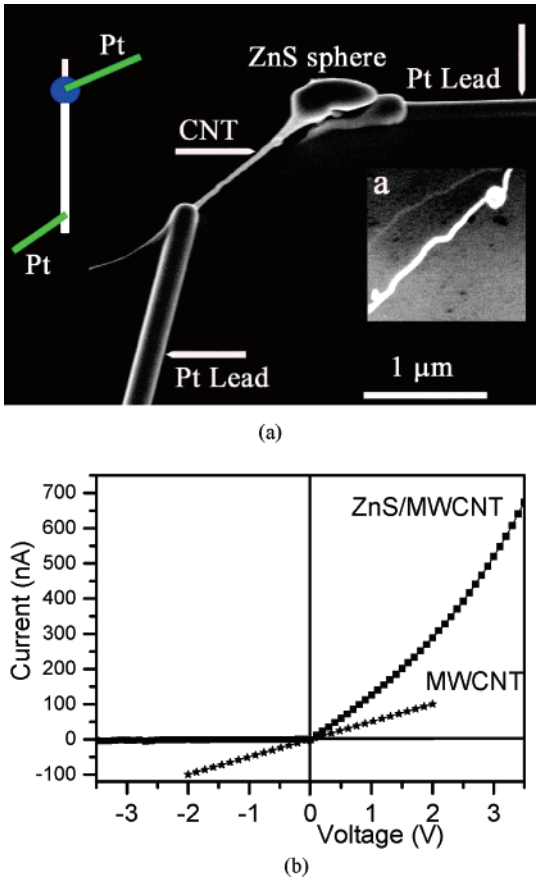

Figure 5. (a) SEM image of an example of MWCNTs/ZnS heterostructures with Pt contacts (the left is the schematic diagram illustrating the framework of the device, and inset a is the SEM image of MWCNTs/ZnS heterostrutures before patterning leads). (b) Current−voltage ($I-V$) characteristics of the MWCNTs/ZnS heterostructures measured at room temperature showing rectifying behavior.

across the junction and is diminished under reverse bias as the potential barrier across the junction increases. Moreover, the electrical properties of our MWCNTs/ZnS heterojunction are very stable in the air. Thus, the MWCNTs/ZnS heterostructures may be used in optical and electronic nanodevices.

Conclusions

The MWCNTs wrapped with ZnS nanospheres can be prepared by a combination of ultrasonic and heat treatments. The formation mechanism for the heterostructrues is discussed on the basis of the experimental results. The MWCNTs/ZnS heterostructures feature a broad blue emission at about 430 nm, indicating that there is a significant ground-state interaction between ZnS nanospheres and MWCNTs. The $I-V$ study of the heterostructures shows clear rectifying behavior. The MWCNTs/ZnS composites have potential applications in different fields, such as in highly efficient photoelectrochemical cells and in microelectronic devices. We believe that the method can also be used to fabricate some other MWCNTs/semiconductor heterostructures.

Acknowledgment. We thank the National Natural Science Foundation of China (50472096, 20133030, 90206049, and 20472089), the Major State Basic Research Development Program, and the Chinese Academy of Sciences.

References and Notes

(1) (a) Favier, F.; Walter, E. C.; Zach, M. P.; Benter, T.; R. Penner, M. *Science* **2001**, *293*, 2227. (b) Li, C.; Zhang, D.; Liu, X.; Han, S.; Tang, T.; Han, J.; Zhou, C. *Appl. Phys. Lett.* **2003**, *82*, 1613.
(2) Kong, J.; Franklin, N. R.; Zhou, C.; Chapline, M. G.; Peng, S.; Cho, K.; Dai, H. *Science* **2000**, *287*, 622.
(3) Cui, Y.; Wei, Q.; Park, H.; Lieber, C. M. *Science* **2001**, *293*, 1289.
(4) Zhang, J.; Sun, L. D.; Jiang, X. C.; Liao, Ch. S.; Yan, C. H. *Cryst. Growth Des.* **2004**, *4*, 309.
(5) Zhu, Y. C.; Bando, Y.; Uemura, Y. *Chem. Commun.* **2004**, 836.
(6) Mailti, A.; Rodriguez, J. A.; Law, M.; Kung, P.; Mckinner, J. R.; Yang, P. *Nano Lett.* **2003**, *3*, 1025.
(7) Sandler, J.; Shaffer, M. S. P.; Prasse, T.; Bauhofer, W.; Schulte, K.; Windle, A. H. *Polymer* **1999**, *40*, 5967.
(8) Wong, E. W.; Sheehan, P. E.; Lieber, C. M. *Science* **1997**, 277.
(9) Silva, L. B. D.; Fagan, S. B.; Mota, R. *Nano Lett.* **2004**, *4*, 65.
(10) Ajayan, P. M. *Chem. Rev.* **1999**, *99*, 1787.
(11) Choi, H. C.; Shim, M.; Bangsaruntip, S.; Dai, H. *J. Am. Chem. Soc.* **2002**, *124*, 9058.
(12) Chen, J.; Liu, H.; Weimer, W. A.; Halls, M. D.; Waldeck, D. H.; Walker, G. C. *J. Am. Chem. Soc.* **2002**, *124*, 9034.
(13) (a) Hirsch, A. *Angew. Chem., Int. Ed.* **2002**, *41*, 1853. (b) Bahr, J.; Tour, J. M. *J. Mater. Chem.* **2002**, *12*, 1952. (c) Kovtyukhova, N. L.; Mallouk, T. E. *Adv. Mater.* **2005**, *17*, 187. (d) Li, X. H.; Niu, J. L.; Zhang, J.; Li, H. L.; Liu, Z. F. *J. Phys. Chem. B* **2003**, *20*, 2453. (e) Ravindran, S.; Bozhilov, K. N.; Ozkan, C. S. *Carbon* **2004**, *42*, 1537. (f) Huang, Q.; Gao, L. *Nanotechnology* **2004**, *15*, 1855.
(14) Haremza, J. M.; Hahn, M. A.; Krauss, T. D. *Nano Lett.* **2002**, *2*, 1253.
(15) Banerjee, S.; Wong, S. S. *Nano Lett.* **2002**, *2*, 195.
(16) Fu, L.; Liu, Z. M.; Liu, Y. Q.; Han, B. X.; Hu, P. A.; Cao, L. C.; Zhu, D. B. *Adv. Mater.* **2005**, *17*, 217.
(17) (a) Kishimoto, S.; Kato, A.; Naito, A.; Sakamoto, Y.; Iida, S. *Phys. Status Solidi* **2002**, *1*, 391. (b) Falconry, C.; Garcia, M.; Ortiz, A.; Alonso, J. C. *J. Appl. Phys.* **1992**, *72*, 1525.
(18) Liang, Q.; Liu, B. C.; Tang, S. H.; Li, Z. J.; Li, Q.; Gao, L. Z.; Zhang, B. L.; Yu, Z. L. *Acta Chim. Sin. (Chin. Ed.)* **2000**, *58*, 1336.
(19) Hu, G.; Cheng, M.; Ma, D.; Bao, X. *Chem. Mater.* **2003**, *15*, 1470.
(20) Wang, W. Z.; Germanenko, I.; EI-Shall, M. S. *Chem. Mater.* **2002**, *14*, 3082.
(21) Cullity, B. D. *Elements of X-ray Diffraction*, 2nd ed.; Addison-Wesley: Menlo Park, CA, 1978.
(22) (a) Li, Y.; Li, X.; Yang, C.; Li, Y. *J. Phys. Chem. B* **2004**, *108*, 16002. (b) Xiong, Q.; Chen, G.; Acord, J. D.; Liu, X.; Zengel, J. J.; Gutierrez, H. R.; Redwing, J. M.; Lew Yan Voon, L. C.; Lassen, B.; Eklund, P. C. *Nano Lett.* **2004**, *4*, 1663.
(23) Zhu, Y. C.; Bando, Y.; Xue, D. F.; Golberg, D. *J. Am. Chem. Soc.* **2003**, *125*, 16196.
(24) Gao, T.; Wang, T. *Chem. Commun.* **2004**, 2558.
(25) Chen, S. W.; Sommers, J. M. *J. Phys. Chem. B* **2001**, *105*, 8816.
(26) (a) Romero, D. B.; Carrard, M.; Zuppiroli, L. *Adv. Mater.* **1996**, *8*, 899. (b) Cao, L.; Chen, H. Z.; Zhou, H. B.; Zhu, L.; Sun, J. Z.; Zhang, X. B.; Xu, J. M.; Wang, M. *Adv. Mater.* **2003**, *15*, 909.
(27) Hago, H.; Shaffer, M. S. P.; Ginger, D. S. *Phys. Rev. B* **2000**, *61*, 2286.
(28) Yan, H. Q.; He, R. G.; Johnson, J.; Law, M.; Saykally, R. J.; Yang, P. D. *J. Am. Chem. Soc.* **2003**, *125*, 4728.
(29) Bhattacharyya, S.; Kymakis, E.; Amaratunga, G. A. J. *Chem. Mater.* **2004**, *16*, 4819.
(30) Cao, J.; Sun, J. Z.; Hong, J.; Li, H. Y.; Wang, H. Z.; Chen, M. *Adv. Mater.* **2004**, *16*, 84.
(31) (a) Tans, S. J.; Verschueren, A. R. M.; Dekker, C. *Nature* **1998**, 393. (b) Misewich, J. A.; Martel, R.; Avouris, P.; Tsang, J. C.; Heinze, S.; Tersoff, J. *Science* **2003**, *300*, 783.
(32) Cui, J. B.; Burghard, M.; Ken, K. *Nano Lett.* **2002**, *2*, 117.
(33) Xiao, K.; Liu, Y.; Hu, P. G.; Yu, F. L.; Zhu, D. B. *Appl. Phys. Lett.* **2003**, *83*, 4824.
(34) Huang, Y.; Duan, X. F.; Cui, Y.; Lieber, C. M. *Nano Lett.* **2002**, *2*, 101.
(35) Zhou, Y.; Gaur, A.; Hur, S.-H.; Kocabas, C.; Meitl, M. A.; Shim, M.; Rogers, J. A. *Nano. Lett.* **2004**, *4*, 2031.
(36) Kong, J.; Dai, H. J. *J. Phys, Chem. B* **2001**, *105*, 2890.